FT-IR Kinetic and Product Study of the OH Radical and Cl-Atom–Initiated Oxidation of Dibasic Esters

FABRIZIA CAVALLI, IAN BARNES, KARL HEINZ BECKER

Bergische Universität–GH Wuppertal, Physikalische Chemie/FB 9, Gauss Strasse 20, D-42097 Wuppertal, Germany

Received 27 July 2000; accepted 28 March 2001

ABSTRACT: Using a relative kinetic technique, rate coefficients have been measured, at 296 ± 2 K and 740 Torr total pressure of synthetic air, for the gas-phase reaction of OH radicals with the dibasic esters dimethyl succinate [$CH_3OC(O)CH_2CH_2C(O)OCH_3$], dimethyl glutarate [$CH_3OC(O)CH_2CH_2CH_2C(O)OCH_3$], and dimethyl adipate [$CH_3OC(O)CH_2CH_2CH_2CH_2C(O)OCH_3$]. The rate coefficients obtained were (in units of cm^3 $molecule^{-1}$ s^{-1}): dimethyl succinate $(1.89 \pm 0.26) \times 10^{-12}$; dimethyl glutarate $(2.13 \pm 0.28) \times 10^{-12}$; and dimethyl adipate $(3.64 \pm 0.66) \times 10^{-12}$. Rate coefficients have been also measured for the reaction of chlorine atoms with the three dibasic esters; the rate coefficients obtained were (in units of cm^3 $molecule^{-1}$ s^{-1}): dimethyl succinate $(6.79 \pm 0.93) \times 10^{-12}$; dimethyl glutarate $(1.90 \pm 0.33) \times 10^{-11}$; and dimethyl adipate $(6.08 \pm 0.86) \times 10^{-11}$. Dibasic esters are industrial solvents, and their increased use will lead to their possible release into the atmosphere, where they may contribute to the formation of photochemical air pollution in urban and regional areas. Consequently, the products formed from the oxidation of dimethyl succinate have been investigated in a 405-L Pyrex glass reactor using Cl-atom–initiated oxidation as a surrogate for the OH radical. The products observed using *in situ* Fourier transform infrared (FT-IR) absorption spectroscopy and their fractional molar yields were: succinic formic anhydride (0.341 ± 0.068), monomethyl succinate (0.447 ± 0.111), carbon monoxide (0.307 ± 0.061), dimethyl oxaloacetate (0.176 ± 0.044), and methoxy formylperoxynitrate (0.032–0.084). These products account for 82.4 ± 16.4% C of the total reaction products. Although there are large uncertainties in the quantification of monomethyl succinate and dimethyl oxaloacetate, the product study allows the elucidation of an oxidation mechanism for dimethyl succinate. Int J Chem Kinet 33: 431–439, 2001

INTRODUCTION

Dibasic esters are currently under consideration as potentially attractive alternatives to established solvents in attempts to introduce low health risk and more environmentally compatible solvents; in particular, compounds that will help to reduce the level of the oxidant formation in the troposphere. Dibasic esters are already employed in a wide variety of applications (coating solvents, paint stripper, plasticizers, polymer intermediates, and resin cleanup), and there could be a significant increase in their usage in the near future. Therefore, because of their possible release into the atmosphere, an evaluation of the atmospheric fate of

Correspondence to: I. Barnes (barnes@physchem.uni-wuppertal.de)

these substances is necessary. To this end, detailed kinetic data and atmospheric reaction mechanistic information are essential in order to be in a position to assess their contribution to the formation of ozone and other photooxidants. To improve our knowledge of the atmospheric chemistry of esters, we report here the results of a kinetic study of the OH radical and chlorine-atom–initiated oxidation of dimethyl succinate [$CH_3OC(O)CH_2CH_2C(O)OCH_3$ DBE-4], dimethyl glutarate [$CH_3OC(O)CH_2CH_2CH_2C(O)OCH_3$ BDE-5], and dimethyl adipate [$CH_3OC(O)CH_2CH_2CH_2CH_2C(O)OCH_3$ DBE-6]. Furthermore, we have investigated the products of the reaction of chlorine atoms with DBE-4 in the presence of NO.

The major atmospheric sink for the dibasic esters is expected to be reaction with OH radicals, which is, however, relatively slow. This makes photoreactor chamber studies of the products difficult because of the long-time coefficients of the experiments required to convert sufficient reactant amounts to the concentrations of products necessary for an accurate analysis. Thus, reaction with chlorine atoms was employed as a surrogate to mimic the OH-radical–induced atmospheric oxidation of dimethyl succinate. Although reaction of VOCs with Cl atoms is somewhat less selective as with OH radicals, the subsequent chemistry is the same and thus it is a convenient method to emulate OH-radical–initiated chemistry.

EXPERIMENTAL

All the experiments were carried out in a 405-L Pyrex cylindrical glass reactor with Teflon-coated metal-end flanges, which has been previously described in detail [1]. A White mirror system mounted inside the reactor and coupled with an external mirror system to a Fourier Transform-Spectrometer (Nicolet Magna 550) enables the *in situ* monitoring of both reactants and products by long-path infrared absorption spectroscopy (total path length 50.4 m). The reactor is equipped with 18 fluorescent lamps (Philips TLA 40W/05, $300 \leq \lambda \leq 450$ nm; $\lambda_{max} = 365$ nm) arranged concentrically around the outside of the chamber and with 3 low-pressure mercury vapor lamps (Philips TUV 40W; $\lambda_{max} = 254$ nm) contained inside an inner quartz glass tube mounted between the centers of the end flanges.

Calibration of dimethyl succinate [$CH_3OC(O)CH_2CH_2C(O)OCH_3$ DBE-4], succinic formic anhydride [$CH_3OC(O)CH_2CH_2C(O)OC(O)H$], monomethyl succinate [$CH_3OC(O)CH_2CH_2C(O)OH$], and dimethyl oxaloacetate [$CH_3OC(O)C(O)CH_2C(O)OCH_3$] was achieved by expanding known amounts of these compounds, dissolved in CH_2Cl_2 or $CHCl_3$, into the evacuated chamber. Quantitative reference spectra of formaldehyde, methoxy formylperoxynitrate, and carbon monoxide were taken from a calibrated infrared spectra data bank archived by this laboratory.

Chemicals

Succinic formic anhydride was synthesized following a procedure similar to that described in the literature for acetic formic anhydride [2]. Briefly, methyl succinyl chloride (Fluka, 98%) was added to finely ground sodium formate (Aldrich, 99%) while the temperature was maintained at 23–27°C with a cooling bath. The mixture was then filtered under suction and the solid residue rinsed with diethylether. After removal of the solvent, succinic formic anhydride, a slightly yellow and viscous liquid, was obtained. The compound had a purity of 90% as determined by NMR.

Dimethyl oxaloacetate (2-oxo-succinic acid dimethyl ester, oxalic acid dimethyl ester) was synthesized according to the following procedure: to a stirred solution of oxalacetic acid (Aldrich, 98%) dissolved in dry methanol, concentrated sulfuric acid was added dropwise. The mixture was heated for a few hours under reflux. The solution was allowed to cool to room temperature, evaporated under vacuum, and redissolved in ethyl acetate. The organic layer was extracted twice with water, using a saturated aqueous solution of NaCl, and dried with anhydrous Na_2SO_4. The removal of the solvent afforded the product, dimethyl oxaloacetate, pure to such an extent that further purification was not necessary.

Dimethyl succinate DBE-4 (98% GC), dimethyl glutarate DBE-5 (98% GC), dimethyl adipate DBE-6 (99+% GC), monomethyl succinate (95%), *n*-butane 2.5 (≥99.5%), ethanol (≥99.8%), 1-propanol (99.5+%), and cyclohexane (99.9+%) were purchased from Aldrich; methyl nitrite was prepared and stored as described by Taylor et al. [3]; Cl_2 (>99.8%), NO (≤99.95%), and synthetic air were supplied by Messer Griesheim.

RESULTS AND DISCUSSION

Rate Coefficients for the Gas-Phase Reactions of Dibasic Esters with OH Radicals and Cl Atoms

Control experiments on each of the three dibasic esters were performed (1) in the dark and (2) at maximum light intensity for up to 40 min to check for losses of reactants via wall adsorption and photolysis, respectively. There were no differences between the loss

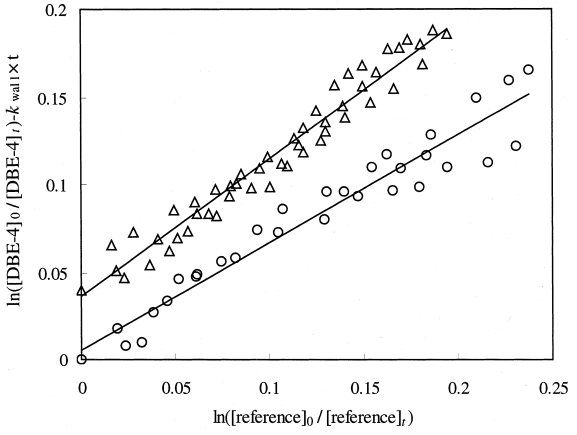

Figure 1 Kinetic data plotted according to eq. (I) from experiments performed in 760 Torr synthetic air at 296 K on the reaction of OH with dimethyl succinate relative to ethanol (circles) and *n*-butane (triangles). The data for the measurement relative to *n*-butane have been displaced vertically by 0.04 units for clarity.

rates observed in the dark and under irradiation conditions, supporting, therefore, that photolysis of the dibasic esters was negligible. Wall loss rates of 5.05×10^{-5} s^{-1}, 5.28×10^{-5} s^{-1}, and 7.03×10^{-5} s^{-1} were measured for DBE-4, DBE-5, and DBE-6, respectively. Rate coefficients for the OH-radical reaction were determined using a relative rate method [4], in which the relative disappearance rates of the dibasic ester and a reference compound, whose OH-radical reaction-rate coefficient is reliably known, were monitored parallel in the presence of OH radicals. Taking into consideration the losses of dibasic esters to the wall of the reactor, the kinetic experimental data can be treated using the following equation:

$$\ln\left\{\frac{[\mathrm{DBE}]_{t_0}}{[\mathrm{DBE}]_t}\right\} - k_{\mathrm{wall}} \times t = \frac{k_{\mathrm{DBE}}}{K_{\mathrm{ref}}} \ln\left\{\frac{[\mathrm{reference}]_{t_0}}{[\mathrm{reference}]_t}\right\} \quad \text{(I)}$$

where $[\mathrm{DBE}]_{t_0}$ and $[\mathrm{reference}]_{t_0}$ are the concentrations of the dibasic ester and the reference compound, respectively, at time t_0; $[\mathrm{DBE}]_t$ and $[\mathrm{reference}]_t$ are the corresponding concentrations at time t; k_{DBE} and k_{ref} are the rate coefficients for the reaction with OH radicals of the dibasic ester and the reference compound, respectively, and k_{wall} is the measured wall loss rate coefficient for the dibasic ester. Typical initial reactant concentrations (in molecule cm^{-3} units) were (2–2.5) × 10^{14} DBE-4; (3–3.5) × 10^{14} DBE-5; and (4–4.5) × 10^{14} DBE-6.

Reaction (1) was measured relative to reactions (4) and (5), reaction (2) was measured relative to reactions (5) and (6), and reaction (3) was measured relative to reactions (6) and (7).

$$\mathrm{OH} + \mathrm{DBE\text{-}4} \rightarrow \mathrm{products} \quad (1)$$

$$\mathrm{OH} + \mathrm{DBE\text{-}5} \rightarrow \mathrm{products} \quad (2)$$

$$\mathrm{OH} + \mathrm{DBE\text{-}6} \rightarrow \mathrm{products} \quad (3)$$

$$\mathrm{OH} + n\text{-}\mathrm{C_4H_{10}} \rightarrow \mathrm{products} \quad (4)$$

$$\mathrm{OH} + \mathrm{C_2H_5OH} \rightarrow \mathrm{products} \quad (5)$$

$$\mathrm{OH} + n\text{-}\mathrm{C_3H_7OH} \rightarrow \mathrm{products} \quad (6)$$

$$\mathrm{OH} + \mathrm{C_6H_{12}} \rightarrow \mathrm{products} \quad (7)$$

The initial concentrations (in molecule cm^{-3} units) of the reference compounds were (4–6) × 10^{14} *n*-C_4H_{10}, (5–9) × 10^{14} C_2H_5OH, (5–9) × 10^{14} *n*-C_3H_7OH, and (1–2) × 10^{14} C_6H_{12}.

OH radicals were generated by the photolysis of between (6–12) × 10^{14} molecule cm^{-3} of methyl nitrite (CH_3ONO) in synthetic air using the fluorescent lamps. Approximately 6 × 10^{14} molecule cm^{-3} of NO was added to the reactant mixtures to suppress the formation of O_3 and NO_3 radicals. In typical kinetic experiments, DBE–methyl nitrite–NO–air mixtures were irradiated for 20 min and 15 spectra were recorded. Four experimental runs were conducted on each dibasic ester–reference pair. The observed disappearance of dimethyl succinate, dimethyl glutarate,

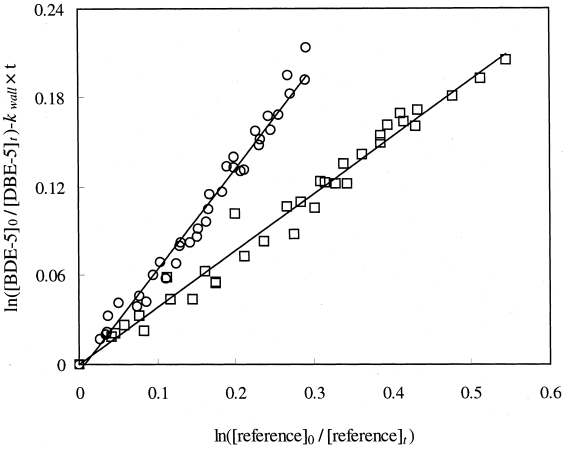

Figure 2 Kinetic data plotted according to eq. (I) from experiments performed in 760 Torr synthetic air at 296 K on the reaction of OH with dimethyl glutarate relative to ethanol (circles) and 1-propanol (squares).

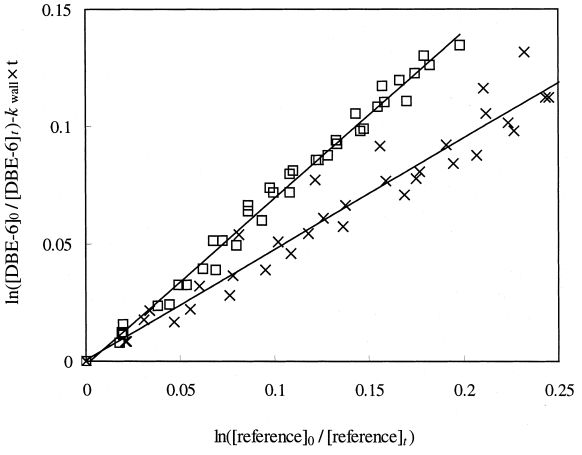

Figure 3 Kinetic data plotted according to eq. (I) from experiments performed in 760 Torr synthetic air at 296 K on the reaction of OH with dimethyl adipate relative to 1-propanol (squares) and cyclohexane (crosses).

and dimethyl adipate, against those of the reference compounds, in the presence of OH radicals, are plotted in Figures 1–3 according to eq. (I). The contribution of the correction for the wall losses, that is, $(k_{wall} \times t)/\{[DBE]_{t_0}/[DBE]_t$, accounts for 25–35% of the measured disappearance of the DBE during the 20-min duration of the experiments. Good straight-line plots were obtained, and the rate coefficient ratios obtained from least-squares analyses of these data are given in Table I. These rate-coefficient ratios have been placed on an absolute basis by use of the following rate coefficients (in cm^3 $molecule^{-1}$ s^{-1} units): $k_4 = 2.44 \times 10^{-12}$ [5], $k_5 = 3.3 \times 10^{-12}$ [6], $k_6 = 5.5 \times 10^{-12}$ [6], and $k_7 = 7.21 \times 10^{-12}$ [5]. The resulting rate coefficients k_1, k_2, and k_3 are given in Table I. The errors indicated for the rate coefficients are 2σ plus an additional uncertainty of 10% due to the potential systematic errors associated with uncertainties in the reference rate coefficient. As seen from Table I, indistinguishable results were obtained from experiments using different reference compounds. We choose to cite final values of k_1, k_2, and k_3 as averages of the individual determinations together with error limits that encompass the extremes of the individual determinations. Hence, $k_1 = (1.89 \pm 0.26) \times 10^{-12}$ cm^3 $molecule^{-1}$ s^{-1}, $k_2 = (2.13 \pm 0.28) \times 10^{-12}$ cm^3 $molecule^{-1}$ s^{-1}, and $k_3 = (3.64 \pm 0.66) \times 10^{-12}$ cm^3 $molecule^{-1}$ s^{-1}. The rate coefficients show the reactivity order, DBE-4 < DBE-5 < DBE-6, that is, an increase in the rate coefficient with an increase in the number of CH_2 groups in the central carbon moiety.

The 298 K rate coefficients were also calculated with the structure–reactivity estimation method of Kwok and Atkinson [7]. The resulting rate coefficients (in cm^3 $molecule^{-1}$ s^{-1} units) are 1.15×10^{-12}, 2.56×10^{-12}, and 3.97×10^{-12} for DBE-4, DBE-5, and DBE-6, respectively, which are in reasonable agreement with the measured values.

Aschmann and Atkinson [8] have recently measured rate coefficients for the reaction of OH radicals with DBE-4, DBE-5, and DBE-6. The reported values (in cm^3 $molecule^{-1}$ s^{-1} units) were: $(1.4 \pm 0.6) \times 10^{-12}$, $(3.3 \pm 1.1) \times 10^{-12}$, and $(8.4 \pm 2.5) \times 10^{-12}$, respectively. Although the rate coefficients measured by Aschmann and Atkinson for DBE-4 and DBE-5 are in reasonable agreement with our measured values, there is a significant discrepancy in the rate coefficient measured for DBE-6 compared to this study. The reason for this large difference is not presently clear. In our experiments, it was generally possible to find IR structural features characteristic only of the DBE reactants and, therefore, to separate them quite accurately from those of the degradation products. However, in the case of the DBE-6, the smooth IR features made a very accurate analysis of the reaction spectra more difficult. The study of Aschmann and Atkinson has, however, also potential problems associated with the analytical procedure used. In particular, the adsorption and thermal desorption employed for the analysis of the dibasic esters could lead to losses of the sticky substrate compounds, especially of those with high boiling point, resulting in larger rate

Table I Kinetic Data for the Reactions of OH Radicals with Dimethyl Succinate, Dimethyl Glutarate, and Dimethyl Adipate Measured at 296 ± 2 K

	$CH_3O(O)CH_2CH_2C(O)OCH_3$		$CH_3O(O)CH_2CH_2CH_2C(O)OCH_3$		$CH_3O(O)CH_2CH_2CH_2CH_2C(O)OCH_3$	
Reference	$k_1/k_{reference}$[a]	k_1[b,c]	$k_2/k_{reference}$[a]	k_2[b,c]	$k_3/k_{reference}$[a]	k_3[b,c]
n-C_4H_{10}	0.78 ± 0.04	(1.90 ± 0.21) × 10^{-12}				
C_2H_5OH	0.59 ± 0.05	(1.88 ± 0.25) × 10^{-12}	0.68 ± 0.03	(2.17 ± 0.24) × 10^{-12}		
n-CH_3H_7OH			0.38 ± 0.02	(2.12 ± 0.24) × 10^{-12}	0.71 ± 0.02	(3.90 ± 0.40) × 10^{-12}
C_6H_{12}					0.47 ± 0.02	(3.38 ± 0.37) × 10^{-12}

[a] Quoted errors are 2σ from a least-squares analysis.

[b] Quoted errors are 2σ plus an additional 10% uncertainty for uncertainties in the reference rate coefficients (see text).

[c] The rate coefficients are given in units of cm^3 $molecule^{-1}$ s^{-1}.

coefficients for the investigated hydroxyl radical reactions.

The rate coefficients measured here can be combined with a diurnally, seasonally, and annually averaged global tropospheric OH radical concentration of 1.0×10^6 molecule cm^{-3} (24-h average) [9] to obtain estimates of the tropospheric lifetimes of the dibasic esters due to gas phase reaction with OH radicals. Using our room-temperature rate constants, the calculated lifetimes range from 6 days for dimethyl succinate to 3 days for dimethyl adipate.

Using the relative rate method and following a similar experimental procedure as described previously for OH, rate coefficients have also been measured for the gas-phase reaction of chlorine atoms with the three dibasic esters, reactions (8) to (10). The reaction of each dibasic ester with Cl was measured relative to chloroethane [CH_3CH_2Cl; reaction (11)] and 2-chloropropane [$CH_3CHClCH_3$; reaction (12)].

$$\text{Cl} + \text{DBE-4} \rightarrow \text{products} \quad (8)$$

$$\text{Cl} + \text{DBE-5} \rightarrow \text{products} \quad (9)$$

$$\text{Cl} + \text{DBE-6} \rightarrow \text{products} \quad (10)$$

$$\text{OH} + \text{CH}_3\text{CHClCH}_3 \rightarrow \text{products} \quad (11)$$

$$\text{Cl} + \text{CH}_3\text{CH}_2\text{Cl} \rightarrow \text{products} \quad (12)$$

The rate constant ratios, in Table II, obtained from least-squares analysis of plots of eq. (I), have been placed on an absolute basis using the following rate constants (in cm^3 molecule^{-1} s^{-1} units): k_{11}(Cl + *iso*-C_3H_7Cl) = 2×10^{-11} [10] and k_{12}(Cl + C_2H_5Cl) = 8.04×10^{-12} [11]. The resulting rate coefficients for the Cl-atom–initiated reaction of DBE-4, DBE-5, and DBE-6 are listed in Table II. Uncertainties quoted for k(Cl + DBE-4), k(Cl + DBE-5), and k(Cl + DBE-6) are 2σ plus an additional 10% uncertainty to account for uncertainties in the reference rate coefficients. As seen from Table II, indistinguishable results were obtained from experiments using different reference compounds. We choose to cite final values for k(Cl + DBE-4), k(Cl + DBE-5), and k(Cl + DBE-6), which are averages of individual determinations with error limits encompassing the extremes of the individual determinations. Hence, k(Cl + DBE-4) = $(6.79 \pm 0.93) \times 10^{-12}$, k(Cl + DBE-5) = $(1.90 \pm 0.33) \times 10^{-11}$, k(Cl + DBE-6) = $(6.08 \pm 0.86) \times 10^{-11}$. Again, the rate coefficients show the expected reactivity order, DBE-4 < DBE-5 < DBE-6, that is, an increase in the rate coefficient with an increase in the number of CH_2 groups in the central carbon moiety.

The chlorine-atom reaction-rate coefficients of the dibasic esters were also calculated using the structure–reactivity relationship method developed by Notario et al. [12]; the calculated values (in cm^3 molecule^{-1} s^{-1} units) k(Cl + DBE-4) = 6.39×10^{-12}, k(Cl + DBE-5) = 2.62×10^{-11}, and k(Cl + DBE-6) = 6.92×10^{-11} are in reasonably good agreement with those measured.

It is interesting at this stage to compare the relative reactivities of OH and Cl with respect to reaction with the dibasic esters investigated in this work. For the OH reactions, the relative reactivities are DBE-4, 1.0; DBE-5, 1.1; and DBE-6, 1.9; but for the Cl reactions, they are DBE-4, 1.0; DBE-5, 2.8; and DBE-6, 8.9. The apparent higher selectivity of Cl atoms toward dimethyl esters than OH radicals can be mainly rationalized in terms of the addition of further CH_2 groups to the central carbon chain of the dibasic esters. In the case of reaction with OH, the addition of further CH_2 groups to the central carbon moiety in DBE-4 only results in modest enhancements to the overall rate coefficient because of the low reactivity of CH_2 groups in this position toward OH. In the case of the Cl reactions, however, the addition of further CH_2 groups results in a large contribution to the overall reactivity because of the very high reactivity of the CH_2 groups in the central position of the molecule toward Cl atoms. Factors such as complex formation, particularly in the case of the OH reactions, may also play a role.

Table II Kinetic Data for the Reactions of Cl Atoms with Dimethyl Succinate, Dimethyl Glutarate, and Dimethyl Adipate Measured at 296 ± 2 K

	$CH_3O(O)CH_2CH_2C(O)OCH_3$		$CH_3O(O)CH_2CH_2CH_2C(O)OCH_3$		$CH_3O(O)CH_2CH_2CH_2CH_2C(O)OCH_3$	
Reference	$k_8/k_{reference}$[a]	k_8[b,c]	$k_9/k_{reference}$[a]	k_9[b,c]	$k_{10}/k_{reference}$[a]	k_{10}[b,c]
C_2H_5Cl	0.87 ± 0.02	$(7.00 \pm 0.72) \times 10^{-12}$	2.19 ± 0.08	$(1.77 \pm 0.19) \times 10^{-11}$	7.80 ± 0.30	$(6.27 \pm 0.67) \times 10^{-11}$
Iso-C_3H_7Cl	0.33 ± 0.01	$(6.58 \pm 0.68) \times 10^{-12}$	1.02 ± 0.02	$(2.03 \pm 0.20) \times 10^{-11}$	2.94 ± 0.10	$(5.88 \pm 0.62) \times 10^{-11}$

[a] Quoted errors are 2σ from a least-squares analysis.

[b] Quoted errors are 2σ plus an additional 10% uncertainty for uncertainties in the reference rate coefficients (see text).

[c] The rate coefficients are given in units of cm^3 molecule^{-1} s^{-1}.

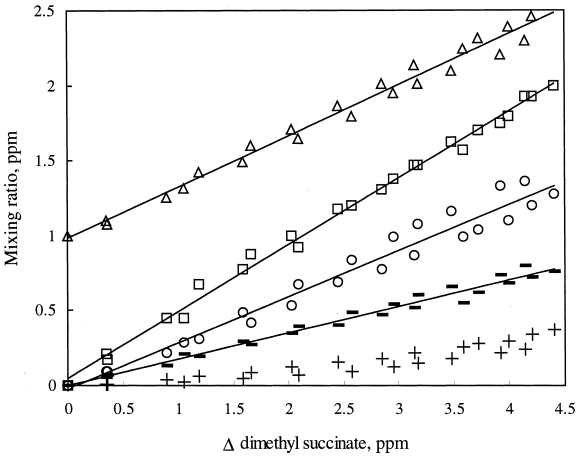

Figure 4 Plots of the amounts of succinic formic anhydride (△), monomethyl succinate (□), CO (○), dimethyl oxaloacetate (−), and methoxy formyl peroxynitrate (+) formed as a function of the amounts of dimethyl succinate reacted with Cl. The data for formic anhydride (△) have been displaced vertically by 1 ppm for clarity.

Product Studies on the Cl-Atom–Initiated Oxidation of Dimethyl Succinate

Photolysis experiments were performed on Cl_2–NO–dimethyl succinate–air mixtures to determine the products formed in the Cl-atom–initiated oxidation of dimethyl succinate. Typical initial concentrations (in units of molecule cm^{-3}) were Cl_2, 6×10^{14}; NO, 6×10^{14}; and dimethyl succinate, 2.5×10^{14}. The mixtures were irradiated for 10 min, and the dimethyl succinate consumption was typically ~60%. Based on FT-IR reference spectra, succinic formic anhydride [$CH_3OC(O)CH_2CH_2C(O)OC(O)H$], monomethyl succinate [$CH_3OC(O)CH_2CH_2C(O)OH$], dimethyl oxaloacetate [$CH_3OC(O)C(O)CH_2C(O)OCH_3$], methoxy formylperoxynitrate [$CH_3OC(O)OONO_2$], and CO were identified among the degradation products. The measured concentrations of these products are plotted as a function of the amounts of dimethyl succinate reacted in Figure 4. Good straight-line plots were obtained; the lack of curvature in the plots strongly supports that all the products are primary and that no secondary reactions generated or removed these reaction products during the time period of the experiments. Least-squares analyses of these data led to the product formation yields given in Table III.

The calibration of monomethyl succinate and dimethyl oxaloacetate were not straightforward because the IR spectra suggested that more than one form of each compound exists in equilibrium in the liquid state and that this equilibrium persists in the gas phase. An attempt was made to obtain an IR spectrum of monomethyl succinate by heating and flushing a solid sample into the evacuated chamber and then filling to atmospheric pressure with synthetic air. No change in the IR features was observed over a time period of 1 h. An attempt was also made to calibrate the solid sample by dissolving it in a solvent, CH_2Cl_2, followed by injection into the chamber. The spectra, in this case, showed with time a slight decrease in the absorption bands of what is most likely the dimer and an increase in the intensities of bands attributed to the monomer. Neither the use of solvents with higher polarity, the heating of the injected solution, nor the increase of the temperature of the reaction chamber resulted in further conversion of the compound to the monomeric form. Therefore, it is not presently possible to ascertain if the calibrated IR spectrum of monomethyl succinate really represents the pure monomeric form or a mixture of the dimer and monomer. An analysis of the product spectra from two experiments afforded an average yield of 0.447 ± 0.111 for methyl succinate. The estimated overall error (25%) includes uncertainties associated with the analysis of the features of monomethyl succinate.

Dimethyl oxaloacetate ester exhibits, as reported in the literature [13], complete enolization in the crystal phase. Being a 1,3-dicarbonyl compound, in solution it exists as an equilibrium mixture of keto and enol forms, the proportionation depending on the polarity of the solvent.

Vapor samples of dimethyl oxaloacetate, introduced into the chamber by heating and flushing samples of the solid with N_2, showed IR features of both keto and enol forms, with an extremely slow conversion rate between the forms compared to the overall dark decay loss to the chamber walls. Therefore, in order to derive a calibrated spectrum for each form, NMR and FT-IR spectra of dimethyl oxaloacetate dissolved in $CDCl_3$ and $CHCl_3$ were recorded over a pe-

Table III Molar Yields of the Products Observed in the Cl-Atom–Initiated Oxidation of Dimethyl Succinate in the Presence of NO_x

Product	Molar Yield
Succinic formic anhydride	0.341 ± 0.068[a]
Monomethyl succinate	0.447 ± 0.111[b]
Carbon monoxide	0.307 ± 0.061[a]
Dimethyl oxaloacetate	0.176 ± 0.044[b]
Methoxy formylperoxynitrate	$0.032 - 0.084$[c]

[a] Errors are the total overall estimated uncertainty of 20%.

[b] Errors are the total overall estimated uncertainty of 25%.

[c] The measured yield depends on the NO/NO_2 ratio in the system.

riod of time of seven days. Both spectra showed complete enolization for the initial freshly prepared solution and, with time, a progressive increase in the fraction of the keto form. Thus, infrared spectra of the pure enol form and then of the equilibrium mixture of the keto and enol forms were obtained. Furthermore, the NMR solution spectra indicated that the position of the keto–enol equilibrium in $CDCl_3$ was 83.5% for the keto form and 16.5% for the enol form. Expansions into the reaction chamber of known amounts of the solution at equilibrium allowed keto and enol infrared absorption bands to be calibrated. As evident from the previous discussion, the FT-IR quantification of monomethyl succinate and dimethyl oxaloacetate is subject to significant uncertainties. Similar difficulties in obtaining IR spectra for the products from DBE-5 (monomethyl glutarate and dimethyl 1,3-acetonedicarboxylate) were observed by Tuazon et al. [14].

In the product spectra, spectral features are observed at 1835, 1748, 1308, 1237, and 799 cm^{-1}. These characteristic absorptions are assigned to methoxy formylperoxynitrate [$CH_3OC(O)OONO_2$]. The formation of this compound is very dependent on the NO/NO_2 ratio in the experimental system and, consequently, its yield is low at the beginning of the experiment when the NO/NO_2 ratio is high and increases gradually during the course of the experiment as the NO/NO_2 ratio becomes smaller (Fig. 4). An estimation of the concentration of the peroxynitrate has been made using the value of 1.09×10^{-3} ppm^{-1} m^{-1} for the absorption cross section of acetylperoxynitrate at 1835 cm^{-1} available in the literature [15]; its yield was found to increase from approximately 3 to 8 mol% during the progression of an experiment. The residual product spectra also show the presence of $RONO_2$-type bands at ~843, ~1298, and ~1679 cm^{-1}. The specific $RONO_2$ products formed could not be identified. However, an estimate of the molar $RONO_2$ concentration was made from the integrated intensity of the 1679 cm^{-1} absorption band and the average integrated absorption coefficient (base 10) of $(2.5 \pm 0.2) \times 10^{-17}$ cm $molecule^{-1}$ of the corresponding band of other organic nitrates [14]. Using this value, the average $RONO_2$ molar formation yield obtained from two experiments was $3.4 \pm 0.6\%$. The estimated total error includes uncertainties associated with the absorption coefficient used and the generally weak signals observed. Model simulations of environmental chamber incremental reactivity experiments [16] involving the reaction of dimethyl succinate with OH radicals in the presence of NO predict overall nitrate yields of ~10–14%.

Since DBE-4 is symmetrical, the chlorine-atom–initiated oxidation can proceed by only two pathways—H-atom abstraction from the terminal methyl groups and H-atom abstraction from the central CH_2CH_2 entity. In the troposphere, the alkyl radicals formed after the H-atom abstractions react solely with O_2 to form the corresponding alkyl peroxy radicals [17]. Further reaction with NO then leads to formation of the analogous alkoxy radicals.

The possible reaction pathways of both alkoxy radicals are outlined in Schemes I and II. The various products identified in the analysis of the IR spectra from the reactions of the two alkoxy radicals are enclosed in boxes in the respective reaction schemes. The products highlighted account for $82.4 \pm 16.4\%$ C.

In the Scheme I, the alkoxy radical $CH_3OC(O)CH_2CH_2C(O)OCH_2O\cdot$ **(I),** formed after the H-atom abstraction at the terminal CH_3 groups of the dibasic ester, undergoes reaction with O_2 to form succinic formic anhydride and an α ester rearrangement to form monomethyl succinate plus the formyl radical, which

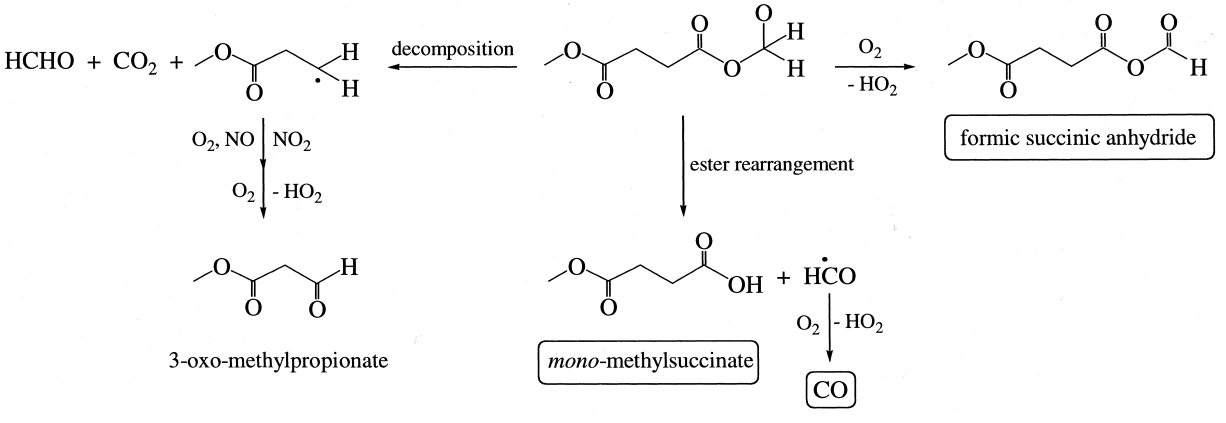

Scheme I Suggested mechanism for the Cl-atom–initiated oxidation of dimethyl succinate; abstraction from the terminal —CH_3 groups.

reacts with O_2 to give CO. If there are no additional sources of CO and monomethyl succinate in the system, as supported by the absence of curvature in plots of their measured concentrations against reacted dimethyl succinate (Fig. 4), then the molar formation yield of the two products should be identical. The observed discrepancy of 14% between the molar formation yield measured for CO and that for monomethyl succinate is very probably attributable to the significant uncertainties in the calibration of the acid. We are, therefore, of the opinion that it is reasonable to assume that the molar formation yield of CO reflects the upper limit for the molar yield formation for monomethyl succinate.

In the FT-IR spectra of the reaction mixture, formation of HCHO was not observed, allowing the decomposition channel of the alkoxy radical $CH_3OC(O)CH_2CH_2C(O)OCH_2O\cdot$ **(I)** to be excluded. This conclusion conforms with similar observations in previous studies on the degradation mechanism of DBE-5 with OH radicals [14] and of methyl propionate with chlorine atoms [18].

In Scheme II, the alkoxy radical $CH_3OC(O)CH(O\cdot)CH_2C(O)OCH_3$ **(II)** formed after H-atom abstraction at the CH_2 groups of DBE-4 can react by four different pathways:

1. Reaction with O_2 will form dimethyl oxaloacetate.
2. Decomposition of this alkoxy radical via C–C cleavage will lead to 3-oxo-methyl propionate plus the methoxy formyl radical ($\cdot C(O)OCH_3$) radical. Under the experimental conditions employed in this study, the major pathway of the $\cdot C(O)OCH_3$ radical is expected to be addition of O_2 and further reaction with NO_2 to form mainly methoxy formylperoxynitrate, rather than decomposition to CO_2 and $\cdot CH_3$ [19]. Because of the lack of a calibrated spectrum for 3-oxomethyl propionate, identification and quantification are not possible; however, the identification of methoxy formylperoxynitrate provides evidence for the occurrence of this pathway.
3. Decomposition of the alkoxy radical $CH_3OC(O)CH(O\cdot)CH_2C(O)OCH_3$**(II)** via C–C cleavage of the central carbon atoms would produce 2 molecules of methyl glyoxylate. However, this channel is obviously of negligible importance because the compound was not observed among the products. This result confirms results from a previous study [16], which deduced that the reaction channel was unimportant because of its relatively high estimated endothermicity.
4. The alkoxy radical $CH_3OC(O)CH(O\cdot)CH_2C(O)OCH_3$ **(II)** can also undergo a 1–5 H shift isomerization through a 6-membered–ring transition state; because of a lack of the spectra of the several possible polyfunctional products, it is not possible to gauge the relative importance of this pathway in the degradation mechanism of dimethyl succinate.

The results of the present investigation have helped to elucidate several aspects of the atmospheric pho-

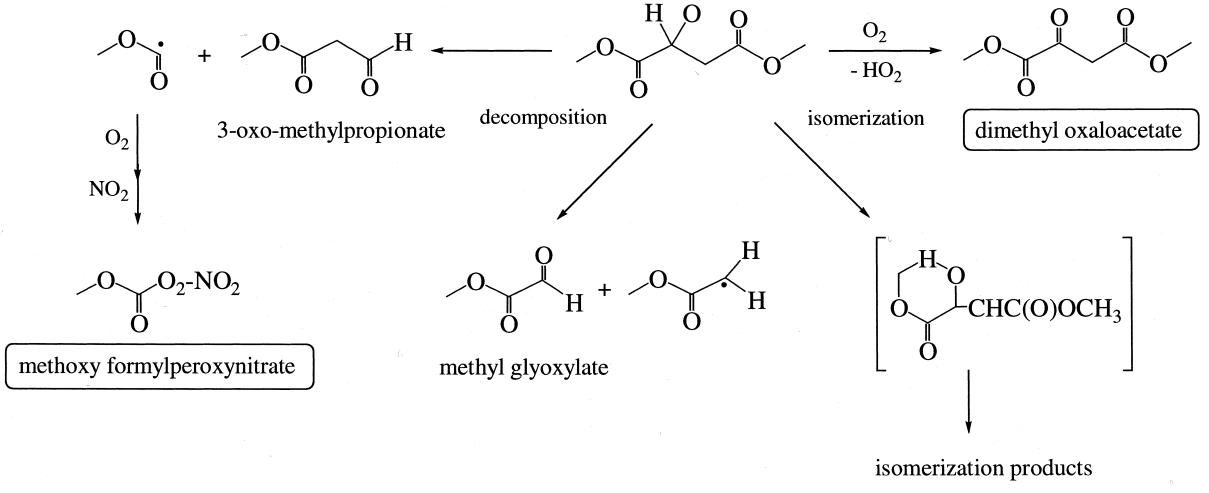

Scheme II Reaction scheme for the Cl-atom–initiated oxidation of dimethyl succinate; abstraction from the central —CH_2CH_2— unit.

tooxidation mechanism of dimethyl succinate. However, the uncertainties encountered in the characterization and quantification of several of the product species demonstrate the need for the use of complementary and interdisciplinary analytical methods to study the complex atmospheric chemistry of larger organic compounds.

F. Cavalli gratefully acknowledges the European Commission for funding her research at the Bergische Universität Wuppertal within the framework of the Environmental and Climate Research and the Specific RTD Program. Financial support within the 4th Framework Program, project EUROSOLV, is also gratefully acknowledged.

BIBLIOGRAPHY

1. Bierbach, A. Produktuntersuchungen und Kinetik der OH-initiierten Gasphasenoxidation aromatischer Kohlenwasserstoffe sowie ausgewählter carbonylischer Folgenprodukte; Ph.D. dissertation, BUGH Wuppertal, Wuppertal, 1994.
2. Krimen, L. I. Org Synth 1970, 50, 1.
3. Taylor, W. D.; Allston, T. D.; Moscato, M. J.; Fezekas, G. B.; Kozlowski, R.; Takacs, G. A. Int J Chem Kinet 1980, 12, 231.
4. Bierbach, A.; Barnes, I.; Becker, K. H.; Wiesen, E. Environ Sci Technol 1994, 28, 715.
5. Atkinson, R. J. Phys Chem Ref Data 1997, 26, 215.
6. Atkinson, R.; Baulch, D. L.; Cox, R. A.; Hampson, R. F., Jr.; Kerr, J. A.; Rossi, M. J.; Troe, J. J. Phys Chem Ref Data 1999, 28, 215, 191.
7. Kwok, E. S. C.; Atkinson, R. Atmos Environ 1995, 29, 1685.
8. Aschmann, S. M.; Atkinson, R. Int J Chem Kinet 1998, 30, 471.
9. Prinn, R. G.; Weiss, R. F.; Miller, B. R.; Huang, J.; Alyea, F. N.; Cunnold, D. M.; Fraser, P. J.; Hartley, D. E.; Simmonds, P. G. Science 1995, 269, 187.
10. Tyndall, G. S.; Orlando, J. J.; Wallington, T. J.; Dill, M.; Kaiser, E. W. Int J Chem Kinet 1997, 29, 43.
11. Wine, P. H.; Semmes, D. H. J Phys Chem 1983, 87, 3572.
12. Notario, A.; Le Bras, G.; Mellouki, A. J Phys Chem 1998, 102, 3112.
13. Schiering, D. W.; Katon, J. E. Spectrochim Acta 1986, 42A, 487.
14. Tuazon, E. C.; Aschmann, S. M.; Atkinson, R. Environ Sci Technol 1999, 33, 2885.
15. Tsalkani, N.; Toupance, G. Atmos Environ 1988, 23, 1849.
16. Carter, W. P. L.; Luo, D.; Malkina, I. L.; Aschmann, S. M.; Atkinson, R. Investigation of the Atmospheric Ozone Formation Potential of Selected Dibasic Esters; Final Report to the Dibasic Esters Group, Synthetic Organic Chemical Manufacturer's Association, 1997. Statewide Air Pollution Research Center, University of California, Riverside (97-AP-RT71-002-FR). http://www.cert.ucr.edu/~carter/bycarter.htm.
17. Atkinson, R. J. Phys Chem Ref Data, Monograph 2, 1994.
18. Cavalli, F.; Barnes, I.; Becker, K. H.; Wallington, T. J. To be published.
19. Maurer, T. Troposphärische Abbaumechanismen ausgesuchter Glykoldiether und Formaldehydacetale; Ph.D. dissertation, BUGH Wuppertal, Wuppertal 2000.